

# Quantized conical waves in multimode optical fibers

Bertrand Kibler and Pierre Béjot\*

*Laboratoire Interdisciplinaire Carnot de Bourgogne, UMR6303 CNRS-UBFC, 21000 Dijon, France*

Multimode optical fibers has emerged as the platform that will bridge the gap between nonlinear optics in bulk media and in single-mode fibers. However, the understanding of the transition between these two research fields still remains incomplete despite numerous investigations of intermodal nonlinear phenomena and spatiotemporal coupling. Some of the striking phenomena observed in bulk media with ultrashort and ultra-intense pulses (i.e., conical emission, harmonic generation and light bullets) require a deeper insight to be possibly unveiled in multimode fibers. Here we generalize the concept of conical waves described in bulk media towards structured media, such as multimode optical fibers, in which only a discrete and finite number of modes can propagate. The modal distribution of optical fibers provides a quantization of conical emission (e.g., quantized X-waves) through phase-matched resonant radiations (i.e., dispersive waves) seeded by optical shocks or ultrashort wave structures during spatiotemporal compression stages. Such quantized dispersion- and diffraction-free waves are generated when a rather intense short pulse propagates nonlinearly in a multimode waveguide, whatever the dispersion regime and waveguide geometry. Future nonlinear experiments in commercially-available multimode fibers could reveal different forms of conical emission and an easy control of supercontinuum light bullets.

DOI:

*Introduction.* The field of nonlinear fiber optics has remained a growing area of research since the end of 1970s [1], in particular sustained and boosted each decade by new technological advances regarding the light pump and the fiber design. In parallel, nonlinear optics in bulk media has also attracted a great deal of attention, through the emergence of intense femtosecond laser sources. In both fields, a strong interest has been manifested in the study of supercontinuum generation taking place during nonlinear pulse propagation [2,3], thus illustrating the connection between the developments of nonlinear optics in fibers and bulks. High powers delivered by femtosecond lasers have allowed to observe a large range of nonlinear optical phenomena in bulk materials [4-7], while single-mode fibers have enhanced nonlinear effects through better light confinement and longer propagation distance [8].

Despite some similarities, single-mode fibers and bulk media have deep intrinsic differences. While an infinite and dense number of transversal modes can propagate in a bulk medium, only one exists in single-mode fibers. Recently, the revival of multimode fibers (MMFs) has led to numerous investigations of intermodal nonlinear phenomena and spatiotemporal coupling, mainly associated with broadband frequency conversion processes [9-10]. As several (quantized) modes propagate in MMFs, such waveguides appear as a relevant intermediate platform for nonlinear optics.

In this context, one can wonder whether nonlinear dynamics observed in bulk media can be transposed to the case of MMFs. For instance, conical emission is one of the striking phenomena observed in bulk samples or condensed media [6]. It is worth to underline that conical emission turns out to be a particular example of conical waves [6-7]. Such fully localized waves have been then

described as non-dispersive and non-diffractive with propagation due to their intrinsic coupled spatiotemporal properties, mainly driven by a phase-matching condition defined by the bulk material dispersion.

In this work, we theoretically and numerically explore nonlinear propagation of ultrashort pulses that drives to similar conical wave phenomena in multimode fibers. The multimode fiber can be considered as an exciting medium, combining bulk and fiber properties to revisit the physics of femtosecond pulse dynamics with new degrees of freedom, in particular by using engineered index profiles and dispersion landscapes, with high-power excitation.

*Theoretical description.* Conical waves are optical wavepackets localized both in space and time which sustain their spatiotemporal shapes during propagation in a bulk medium [6,11]. This property results from their intrinsically coupled spatiotemporal structures by which the combined effects of spatial diffraction and temporal dispersion cancel each other. In particular, nonlinear conical waves have been shown to spontaneously emerge during the propagation of ultrashort and ultra-intense laser pulses in bulk media [6,12-15]. In general, conical emission observed during the filamentation process is nothing but the manifestation of X-wave generation. Conical waves can either take the form of a hyperbola (X-wave) or an ellipse (O-wave), as well as their combination (Fish-wave), in the  $(k_{\perp}, \omega)$  plane, where  $k_{\perp}$  is the transversal component of the wave vector and  $\omega$  the frequency ( $\omega_0$  the carrier frequency). This simply depends on pulse propagating in the normal or the anomalous dispersion regime. While a dense number of modes can propagate within a bulk medium, structured and/or finite media (i.e., waveguides)

support only a discrete number of modes at a given frequency  $\omega$  that can propagate within the waveguide core. Note however, that the combination of core-guided, cladding-guided and evanescent modes forms an (infinite) orthogonal basis set in which any electric field  $E$  can be decomposed as follows:

$$E(r, t, z) = \int \sum_{m=1}^{\infty} \bar{E}(m, \omega) \mathcal{F}(r, m, \omega) e^{-i\omega t} d\omega \quad (1)$$

where  $\mathcal{F}(r, m, \omega)$  is the transversal shape of the mode  $m$  for a given  $\omega$ .

The unidirectional pulse propagation equation generalized to structured media (i.e., media embedding a transversal distribution of the refractive index) expressed in the modal basis reads in the linear regime as:

$$\partial_z \bar{E}(m, \omega) = i K_z(m, \omega) \bar{E}(m, \omega) \quad (2)$$

where  $\bar{E}(m, \omega)$  is the electric field coordinate on the mode  $m$  at a frequency  $\omega$  and  $K_z$  is the propagation constant of the mode  $m$  at a given  $\omega$ . Writing the electric field

$E(r, t, z) = A(r, t, z) e^{i(K_z^{(0)} z - \omega_0 t)}$  and considering a frame propagating at the group velocity  $1/K_z^{(1)}$ , where  $K_z^{(0)} = K_z(1, \omega_0)$  and  $K_z^{(1)} = \{\partial_\omega K_z(1, \omega)\}_{\omega=\omega_0}$ , one obtains the following unidirectional pulse propagation equation:

$$\partial_z \bar{A}(m, \omega - \omega_0) = i [K_z(m, \omega - \omega_0) - K_z^{(0)} - K_z^{(1)}(\omega - \omega_0)] \bar{A}(m, \omega - \omega_0) \quad (3)$$

One can define families of modes that all satisfy the same relation:

$$K_z(m, \omega - \omega_0) - K_z^{(0)} - K_z^{(1)}(\omega - \omega_0) = \delta K_z^{(0)} - \delta K_z^{(1)}(\omega - \omega_0) \quad (4)$$

where  $\delta K_z^{(0)}$  and  $\delta K_z^{(1)}$  are arbitrarily chosen constants. Any superposition of modes belonging to a given family forms a wavepacket localized in both space and time, propagating without any distortion at a group velocity  $1/(K_z^{(1)} + \delta K_z^{(1)})$ . Note that Eq. (4) is also valid for bulks. However, in the latter case, at any  $\omega$  corresponds a value of  $k_\perp$  (since the latter can take any value) for a given family of conical waves [16]. This is not true anymore in the context of quantized conical waves generated in waveguides. Indeed, the family of transversal modes propagating in the waveguide core is discrete. As a result, only a discrete number of frequencies (denoted hereafter  $\Omega_m = \omega_m - \omega_0$ ) satisfy the relation (4).

The electric field component of a quantized conical wave is then composed of delta functions:

$$\bar{E}(m, \omega) = \bar{\epsilon}(m) \delta(\omega - \omega_m) \quad (5)$$

In the temporal domain, the envelope of a quantized conical wave then reads:

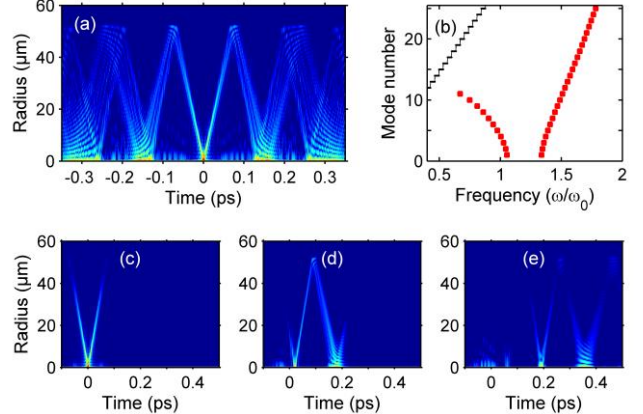


FIG. 1. Example of conical wave emission in a step-index MMF. (a) Full spatiotemporal power (over 4 decades). (b) Modal distribution of phase-matched frequencies (red squares). Black curve: number of guided modes. (c-e) Evolution of a realistic (i.e., dispersive) ultrashort (80-fs duration) conical wave with propagation distance (for  $z = 0, 1$ , and 3 mm, respectively).

$$A(r, t) = \sum_{m=1}^{\infty} \bar{\epsilon}(m) \mathcal{F}(r, m, \omega_m) e^{-i\Omega_m t} \quad (6)$$

Since the conical wave follows Eq. (4), its complex amplitude will evolve during the propagation as:

$$A(r, t, z) = \sum_{m=1}^{\infty} \bar{\epsilon}(m) \mathcal{F}(r, m, \omega_m) e^{-i[\Omega_m t - (\delta K_z^{(0)} + \delta K_z^{(1)} \Omega_m) z]} \quad (7)$$

The resulting localized wavepacket formed by the superposition of modes is not impacted by the propagation; its invariant intensity shape directly depends on the phase-matched frequencies from Eq. (4) and waveguide properties. In Fig. 1(a), an example of quantized conical wave is numerically reconstructed in the space-time domain, by using the MMF parameters studied in the next section. In particular, we considered the X-shaped pattern of the field distribution in the  $(m, \omega)$  domain (see red squares in Fig. 1(b)), when pumping in the normal dispersion regime. The corresponding  $(r, t)$  pattern is characterized by a quasi-periodicity and a central V-shaped structure that exhibits a peak in the radial center (see Fig. 1(a)). Two symmetric decaying tails define a spatiotemporal cone vanishing at the core-clad interface of the waveguide.

In practice, a quantized conical wave has a finite energy, and then cannot contain only purely monochromatic components. All modes involved will rather have a non-zero spectral width. A more realistic conical wave will then write as Eq. (1) with  $\bar{E}(m, \omega)$  a relatively narrow function centered on  $\omega_m$  representing the spectral complex amplitude of the conical wave component whose carrier frequency oscillates at  $\omega_m$  in the  $m^{\text{th}}$  mode. As a consequence, the temporal complex amplitude  $A(r, t)$  of a conical wave can be well approximated by

$$A(r, t) = \sum_{m=1}^{\infty} a_m(t) \mathcal{F}(r, m, \omega_m) e^{-i\Omega_m t} \quad (8)$$

where  $a_m(t)$  is the temporal envelope of the component in the  $m^{\text{th}}$  mode at a carrier frequency  $\omega_m$ . Accordingly, its complex amplitude will evolve during the propagation as:

$$A(r, t, z) = \sum_{m=1}^{\infty} a_m(t - (K_{z(m, \omega_m)}^{(1)} - K_{z(1, \omega_0)}^{(1)})z) \mathcal{F}(r, m, \omega_m) e^{-i[\omega_m t - (\delta K_z^{(0)} + \delta K_z^{(1)} \omega_m)z]} \quad (9)$$

Then, the temporal envelope of the modes composing the conical wave (i.e., a broadband ultrashort pulse structure) does not propagate at the same group velocity. The propagation leads to a temporal dispersion of the conical wave, as depicted in Fig. 1(c-e), which depends on the spectral width of each component.

*Numerical simulations and results.* Our numerical approach of nonlinear pulse propagation in MMFs is based on the multimode unidirectional pulse propagation equation (MM-UPPE) recently derived in Ref. [17], which describes the evolution of the complex electric field in the scalar approximation:

$$\partial_z \bar{A} = i \left[ K_z - K_{z(1, \omega_0)}^{(1)} (\omega - \omega_0) \right] \bar{A} + \frac{i n_0 n_2 \omega^2}{c^2 K_z} \{ (1 - f_R) \bar{|A|^2} \bar{A} + f_R \bar{\int h_R(\tau) |A(t - \tau)|^2 d\tau} \bar{A} \}, \quad (10)$$

where  $n_0$  is the core refractive index calculated at  $\omega_0$ , the pump frequency.  $n_2 = 3.2 \times 10^{-20} \text{ m}^2 \text{ W}^{-1}$  is the nonlinear refractive index of silica glass [1]. The function  $h_R$  is the Raman response with fraction  $f_R = 0.18$  for fused silica glass. The propagation equation is expressed in a retarded frame moving at velocity  $1/K_{z(1, \omega_0)}^{(1)}$ . As described in Ref. [17], both the propagation constants and transverse distributions of the (frequency dependent) modes can be calculated by operating a diagonalization of the operator describing the propagation  $[\Delta_{\perp} + n^2(r, \omega) \omega^2/c^2]$ . We solve the propagation by a split-step algorithm during which the linear term is evaluated within the modal basis while the nonlinear step is calculated in the  $(r, t)$  space.

In the following, we compare the numerical results with our theoretical approach to unveil the formation of quantized conical waves in MMFs, more specifically in the case of femtosecond pulse pumping and input peak powers around the critical self-focusing threshold of silica glass. We first investigate the nonlinear propagation of 100-fs Gaussian pulses injected into the fundamental mode of a 4-cm-long segment of standard step-index MMF. The pump pulse is fixed at  $\lambda_0 = 800 \text{ nm}$ , in the normal dispersion regime of the fiber. The fiber under study exhibits typical features of commercially-available MMFs (pure silica core with diameter  $\phi = 105 \text{ } \mu\text{m}$ , and numerical aperture  $NA = 0.22$ ). Our scalar approach limited our studies to the linearly polarized modes of  $LP_{0,n}$  class. As the considered fiber is circularly symmetric, the coupling coefficients are

nonzero only for  $LP_{0,n}$  modes, when pumping configuration is a beam coupling into the fundamental mode of the fiber (namely  $LP_{0,1}$  mode). Note that the effect of usual fiber losses (less than 10 dB/km) is found here to be negligible.

Figure 2(a) shows the distribution of the full optical spectrum (power in log. scale) over the different fiber modes after 4 cm of propagation. We observe here an evident X-shaped pattern of the field distribution that is very similar to one typical example of conical waves (X waves) well studied in the Fourier  $(k_{\perp}, \omega)$  domain for bulk media [6]. The spontaneous formation of this energy spreading in higher-order modes from the fundamental mode can be retrieved by using the theoretical relation (4) of quantized conical waves (see white squares). We confirm the formation of a quantized conical wave for which the blue and highest frequencies are continuously contained in higher-order modes. Note that it is also possible to transform our specific mode-frequency representation of Fig. 2(a) for waveguides into the full Fourier  $(k_{\perp}, \omega)$  domain. We would obtain the similar X-shape signature since higher-order modes contains the highest spatial frequencies (conical tails exhibit an increasing transverse wavenumber with frequency detuning).

The detailed nonlinear propagation for power spectrum, time and space profiles are shown in Figs. 2(b)-2(d), respectively. We observe that the spectral dynamics reaches a stationary state after 1.2 cm (see Fig. 2(b)), just past the pulse splitting phenomenon observed in the time domain. We then globally retrieve a typical scenario already analyzed in normal dispersion of bulk media, namely, the self-focusing dynamics and spectral broadening are associated to pulse splitting phenomena [7,18]. The pulse splitting occurring at the nonlinear spatial focus produces two sub-pulses moving in opposite directions in our retarded time frame (see Fig. 2(c)). As depicted in Fig. 2(e-f), we notice a strong and rapid spectral broadening at 1 cm induced by the self-steepening effect. In particular, the velocity difference between the trailing pulse peak and its tails leads to the formation of an optical shock (at the trailing edge) due to the nonlinear dependence of the refractive index. The shock front on the trailing edge is then followed by wave-breaking. The simultaneous strong broadening seeds linear waves, which are resonantly amplified in higher order modes according to the velocity of the shock front. This simply corresponds to phase-matched resonant radiations over the fiber modes (i.e., a quantized X-wave is formed), mainly satisfying the group velocity of the shock front as described by our relation (4). More specifically,  $\delta K_z^{(1)}$  can be found through the group velocity difference between the shock front and  $1/K_{z(1, \omega_0)}^{(1)}$ , whereas  $\delta K_z^{(0)}$  is governed by the nonlinear contribution to the phase velocity.

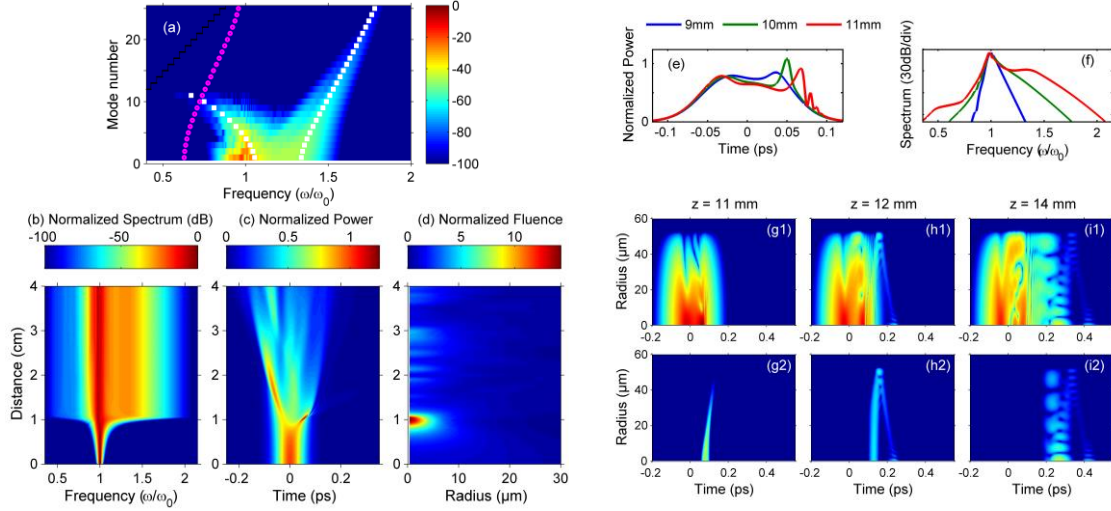


FIG. 2. Nonlinear propagation of 100-fs pulses (300-nJ energy at 800 nm) in a 4-cm-long segment of step-index MMF. (a) Output modal distribution of the power spectrum. White squares: theoretical phase-matched frequencies of the quantized conical wave. Black curve: number of guided modes. Magenta circles: zero-dispersion frequency for each guided mode. (b-d) Evolution of the normalized full power spectrum, instantaneous power, and fluence with propagation distance, respectively. (e-f) Snapshots of temporal and spectral power profiles showing the optical shock formation and strong spectral broadening. (g1-i1) Evolution of the full spatiotemporal power distribution (over 6 decades) for distinct propagation distances. (g2-i2) Corresponding evolution for the filtered high-frequency tail of X-pattern from  $(m, \omega)$  plane.

Next, we unveil the formation of the conical wave in the direct  $(r, t)$  space, in particular at the trailing edge (see Fig. 2(g1-i1)). A simple spectral filtering procedure of one tail of the X pattern from Fig. 2(a) allowed us to reveal its location and shape in the  $(r, t)$  space (see Fig. 2(g2-i2)). We clearly retrieve the spatiotemporal signatures of the theoretical solution (9) illustrated in Fig. 1, namely half of the cone emitted at the shock front position and then propagating into the fiber core in a dispersive manner. Note that several analytical shapes of localized waves of the conical type have already been analyzed and classified for bulk media as a function of the dispersive properties of the medium [19-20], this could also be done for any fiber design.

Overall, the dynamics above-observed in MMFs recalls the interplay between shock front (axial spectral broadening) and X-wave formation (conical spectral broadening) in a similar way to shocked-X wave dynamics described in femtosecond filamentation [21]. Moreover, it also makes the connection with well-known dynamics of dispersive shock waves studied in single-mode fibers which results in the emission of resonant radiations by the same phase-matching rule as our relation (4), but restricted to the fundamental mode [22]. The condition (4) can be seen as a generalized phase-matching rule of resonant radiations emitted by a broadband localized structure (soliton, shock front) through intra- and inter-modal properties of any waveguide and whatever the dispersion regime.

To this regard, we next investigate nonlinear propagation in the anomalous dispersion regime of the MMF, namely by pumping at  $\lambda_0 = 1400$  nm. Figure 3(a)

depicts the corresponding distribution of the full optical spectrum (power in log. scale) over the different fiber modes after 4 cm of propagation. A combination of both X-wave and O-wave is obtained in the  $(m, \omega)$  plane, also known as a Fish-wave pattern. This spontaneous reshaping results from the large spectral broadening that covers both normal and anomalous dispersion regimes. Again, we are able to retrieve the corresponding quantized conical wave (by using the theoretical relation (4)), which is characterized by only one tail of the X-wave at high frequencies and the O-wave at low frequencies. If looking at the propagation details for spatial, temporal, and spatial profiles (not presented here), we would note a main pulse splitting phenomenon leading to the half X-wave pattern. We also checked that pumping farther from the zero dispersion (e.g., at  $\lambda_0 = 1800$  nm) would result in the quantization of a single nonlinear O-wave (i.e. light bullet) similar to previous studies in bulk media [23].

In addition, we present numerical results obtained in the case of a 2-cm-long segment of gradient-index (GRIN) MMF pumped at  $\lambda_0 = 800$  nm (see Fig. 3(b)). We consider a typical  $\text{GeO}_2$ -doped core with a diameter of 105- $\mu\text{m}$  and a parabolic index profile, as well as a numerical aperture  $NA = 0.2$ . Figure 3(b) shows an evident X-shaped pattern of the field distribution over guided modes, but slightly different from the case of step-index MMFs. In particular, we observe distinct curvatures of conical tails spreading in higher-order modes. This specific behavior obtained in GRIN fibers is predicted by theoretical relation (4) of quantized conical waves (see white squares). It would also lead to another type of conical emission in the  $(r, t)$  space.

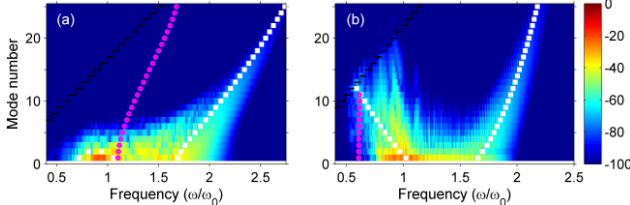


FIG. 3. (a) Same step-index MMF as in Fig. 1 with 450-nJ 100-fs pumping at 1400 nm. Output modal distribution of the power spectrum after 4 cm of propagation. (b) Output modal distribution of the power spectrum obtained from nonlinear propagation of 100-fs pulses (210-nJ energy at 800 nm) coupled into the  $LP_{0,1}$  mode of a 2-cm-long GRIN fiber.

The evolution of spectral, temporal and spatial profiles with propagation (not presented here) indicates the saturation of the spectral broadening after 5 mm, just past the first successive and periodic pulse splitting phenomena observed in the time domain associated to periodic self-imaging of GRIN fibers [24].

For the sake of clarity, we have only studied the fundamental mode excitation with femtosecond pulses. However, supercontinuum studies in single-mode fibers have demonstrated that the long-pulse pumping regime also lead to the emergence of ultrashort pulses and dispersive waves through an intermediate stage of modulation instability (MI) [3]. In the case of MMFs, various forms of MI can be observed [10] and considered as intermediate nonlinear processes possibly seeding a set of resonant radiations forming a quantized conical wave. Besides, the impact of spatial excitation still needs to be studied, for instance a simple multimode excitation by means of a large Gaussian beam. This typical pumping configuration was studied experimentally in several previous works [25-27], in particular for GRIN fibers. Such fibers exhibit well-confined fundamental guided modes in strong contrast to step-index fibers, the latter class of MMFs then appears as better candidates for future experimental demonstration of quantized conical wave formation.

*Conclusion.* In summary, we reported on the theoretical description and numerical observation of quantized conical wave formation in MMFs, which is described by a superposition of phase-matched resonant radiations seeded by ultrashort pulse structures. The discrete modal distribution of multimode waveguides then provides a quantization of the well-known conical emission in bulk media. The rich phase-matching landscape of such waveguides, for instance commercially-available MMFs, implies that various types of quantized conical waves can be observed whatever the dispersion regime and waveguide geometry. Our study opens the way for further fundamental investigations and nonlinear experiments that complete the transition between nonlinear optics in bulk media and in single-mode fibers.

*Acknowledgments.* We acknowledge financial support of the French “Investissements d’Avenir” program (PIA2/ISITE-BFC, contract ANR-15-IDEX-03; EIPHI Graduate School, contract ANR-17-EURE-0002). The authors thank K. Tarnowski and S. Majchrowska for stimulating discussions. Calculations were performed using HPC resources from DNUM-CCUB (Université de Bourgogne).

\* [pierre.bejot@u-bourgogne.fr](mailto:pierre.bejot@u-bourgogne.fr)

- [1] G. P. Agrawal, *Nonlinear Fiber Optics – 6<sup>th</sup> Ed.*, Academic Press, London, 2019.
- [2] R. R. Alfano, *The Supercontinuum Laser Source, The Ultimate White Light – 3<sup>rd</sup> Ed.*, Springer, New York, 2016.
- [3] J. M. Dudley, G. Genty, and S. Coen, *Rev. Mod. Phys.* **78**, 1135 (2006).
- [4] R. R. Alfano and S. L. Shapiro, *Phys. Rev. Lett.* **24**, 584 (1970).
- [5] R. R. Alfano and S. L. Shapiro, *Phys. Rev. Lett.* **24**, 592 (1970).
- [6] D. Faccio, A. Couairon, and P. Di Trapani, *Conical Waves, Filaments and Nonlinear Filamentation Optics*, Aracne, Roma, 2007.
- [7] A. Dubietis and A. Couairon, *Ultrafast Supercontinuum Generation in Transparent Solid-State Media*, Springer Nature, Cham, 2019
- [8] R. H. Stolen, *J. Light. Technol.* **26**, 1021 (2008).
- [9] L. G. Wright, D. N. Christodoulides, and F. W. Wise, *Nat. Photon.* **9**, 306 (2015).
- [10] K. Krupa, A. Tonello, A. Barthélémy, T. Mansuryan, V. Couderc, G. Millot, P. Grelu, D. Modotto, S. A. Babin, and S. Wabnitz, *APL Photonics* **4**, 110901 (2019).
- [11] H. Sönajalg, M. Rätsep, and P. Saari, *Opt. Lett.* **22**, 310 (1997).
- [12] C. Conti, S. Trillo, P. Di Trapani, G. Valiulis, A. Piskarskas, O. Jedrkiewicz, and J. Trull, *Phys. Rev. Lett.* **90**, 170406 (2003).
- [13] M. Kolesik, E. M. Wright, and J. V. Moloney, *Phys. Rev. Lett.* **92**, 253901 (2004).
- [14] M. A. Porras, A. Parola, and P. Di Trapani, *J. Opt. Soc. Am. B* **22**, 1406 (2005).
- [15] D. Faccio, M. A. Porras, A. Dubietis, F. Bragheri, A. Couairon, and P. Di Trapani, *Phys. Rev. Lett.* **96**, 193901 (2006).
- [16] In the case of bulk materials, the propagation constant writes  $K_z = \sqrt{k^2(\omega) - k_\perp^2}$ . In first approximation and in the case  $\delta K_z^{(0)} = \delta K_z^{(1)} = 0$ , Eq. (4) then reduces to  $k_\perp = \sqrt{k_0 k^{(2)} |\omega|}$ , where  $k_0$  and  $k^{(2)}$  are the wavenumber and the second-order dispersion at the central frequency, respectively.
- [17] P. Béjot, *Phys. Rev. E* **99**, 032217 (2019).
- [18] J. K. Ranka, R. W. Schirmer, and A. L. Gaeta, *Phys. Rev. Lett.* **77**, 3783 (1996).

- [19] S. Malaguti and S. Trillo, Phys. Rev. A **79**, 063803 (2009).
- [20] A. Lotti, A. Couairon, D. Faccio, and P. Di Trapani, Phys. Rev. A **81**, 023810 (2010).
- [21] F. Bragheri, D. Faccio, A. Couairon, A. Matijosius, G. Tamošauskas, A. Varanavičius, V. Degiorgio, A. Piskarskas, and P. Di Trapani, Phys. Rev. A **99**, 025801 (2007).
- [22] S. Trillo and M. Conforti, *Wave-Breaking and dispersive Shock Wave Phenomena in Optical Fibers*, in Shaping Light in Nonlinear Optical Fibers (eds C. Finot, S. Boscolo), Wiley, Chichester, 2017.
- [23] D. Majus, G. Tamošauskas, I. Gražulevičiūtė, N. Garejev, A. Lotti, A. Couairon, D. Faccio, and A. Dubietis, Phys. Rev. Lett. **96**, 193901 (2006).
- [24] G. P. Agrawal, Opt. Fib. Tech. **50**, 309 (2019).
- [25] L. G. Wright, S. Wabnitz, D. N. Christodoulides, and F. W. Wise, Phys. Rev. Lett. **115**, 223902 (2015).
- [26] K. Krupa, A. Tonello, A. Barthélémy, V. Couderc, B. M. Shalaby, A. Bendahmane, G. Millot, and S. Wabnitz, Phys. Rev. Lett. **116**, 183901 (2016).
- [27] M. A. Eftekhar, L. G. Wright, M. S. Mills, M. Kolesik, R. Amezcua Correa, F. W. Wise, and D. N. Christodoulides, Optics Exp. **25**, 9078 (2017).